Electronic Band Structure of $GaN_xP_yAs_{1-x-y}$ Highly Mismatched Alloys: Suitability for Intermediate-Band Solar Cells

R. Kudrawiec,[1,2*] A. V. Luce,[1,3] M. Gladysiewicz,[2] M. Ting,[4] Y. J. Kuang,(邝彦瑾)[5] C. W. Tu,[6] O. D. Dubon,[1,3] K. M. Yu,[1] and W. Walukiewicz[1]

[1]*Materials Sciences Division, Lawrence Berkeley National Laboratory, Berkeley, California 94720, USA*
[2]*Institute of Physics, Wroclaw University of Technology, Wybrzeze, Wyspianskiego 27, 50-370 Wroclaw, Poland*
[3]*Department of Materials Science and Engineering, University of California, Berkeley, California 94720, USA*
[4]*Department of Mechanical Engineering, University of California, Berkeley, California 94720, USA*
[5]*Department of Physics, University of California, San Diego, La Jolla, California 92093, USA*
[6]*Department of Electrical and Computer Engineering, University of California, San Diego, La Jolla, California 92093, USA*

(Received 6 February 2014; published 28 April 2014)

Formation of an intermediate band in $GaN_xP_{0.4}As_{0.6-x}$ alloys due to the isovalent doping by nitrogen is studied by photoreflectance and absorption spectroscopy. The fundamental energy gap transition (E_0) observed for an N-free alloy is replaced by two optical transitions (E_- and E_+) in GaNPAs layers. The E_- and E_+ transitions are explained within the band anticrossing model, where the localized level of nitrogen interacts with the conduction band of the GaPAs host, splitting it into two subbands. The valence band (VB) is mostly unaffected by nitrogen incorporation as confirmed by the same spin-orbit splitting for N-free and N-containing alloys. The energy position of the E_- subband and a strong optical absorption between the VB and the E_- subband indicates the GaNPAs alloys have an electronic structure suitable for intermediate-band solar cells. Such an electronic structure is not observed for other III–V alloys like GaInAs, GaInAsP, etc., for which the virtual crystal approximation can be applied to describe the evolution of the electronic structure with the alloy content. Results obtained in this work clearly show that GaNPAs with a few percent of nitrogen is an unusual material system, for which the electronic structure properties differ very significantly from properties of well-known III–V alloys, and the application of virtual crystal approximation in this case is inappropriate or very limited.

DOI: 10.1103/PhysRevApplied.1.034007

I. INTRODUCTION

Highly mismatched alloys (HMAs) are a class of semiconductors in which one or more of the component elements are replaced with elements of much different size and/or electronegativity [1–5]. The electronic band structure of HMAs is well described by the band anticrossing (BAC) model that describes the interaction of the extended band states of the host material with localized states introduced by the minority component of the alloy. In its original formulation, the BAC model was applied to calculate effects of the interaction between the extended conduction band (CB) states of GaAs with localized N states in GaNAs alloys with small N content [1]. It was later generalized to consider cases in which localized states of the minority elements affect the valence band structure [6]. One of the striking features of HMAs is that the BAC interaction leads to the formation of new electronic bands separated from the bands of the host matrix. This discovery creates a potential for using HMAs in intermediate-band solar cells (IBSCs), a new type of cell that can more efficiently utilize the full solar spectrum [7–9]. Theoretical calculations show that the maximum efficiency for IBSCs under idealized conditions requires a band gap of 1.95 eV that is split into two subbands of 0.71 and 1.24 eV [7,8]. The first IBSC utilizing a HMA was fabricated by using a GaNAs alloy to demonstrate the working principle of the concept [10]. Further illustrations of the feasibility of the HMAs for IBSC application are provided by experiments on GaNAs(Sb) [11] as well on ZnOTe [12]. However, in all these cases the width and/or locations of the bands do not satisfy the optimum band gap distribution. In particular, in GaNAs, since the IB is derived from the original CB of GaAs, the IB is relatively wide and not entirely separated from the CB. On the other hand, a narrow, separated IB can be formed only if the localized states occur well below the CB as in the case of ZnOTe [9]. However, *n*-type doping of ZnOTe is still a challenging task. Therefore, there is a need for a material system that can be doped both *n* and *p* type with additional control of the band edge energies as well as density of states for IBSCs with maximum power conversion efficiency.

*r.kudrawiec@lbl.gov, robert.kudrawiec@pwr.wroc.pl

In this paper, we report a comprehensive theoretical and experimental study of the $GaN_xP_yAs_{1-y-x}$ (with $y \sim 0.4$) HMA. We show that this alloy with up to 2% of nitrogen has an electronic band structure optimized for intermediate-band solar cell applications. The paper is organized as follows: Sec. II presents the calculations of the electronic structure of GaNPAs using the BAC model; measurements of optical transition energies in GaNPAs alloys with various N and P concentrations are compared with the theoretical predictions in Sec. III.

II. THEORY

The unusual behavior of the band structure of III–V semiconductors upon incorporation of nitrogen (such as the dilute nitrides) is documented by many experimental studies including photoreflectance (PR) measurements of optical transitions at the Γ point [1,13–19]. The most important observations from these studies are that (i) nitrogen strongly reduces the fundamental energy gap, (ii) an extra higher-energy optical transition at the Γ point is observed for N-containing alloys [1,13–19], and (iii) the spin-orbit splitting does not depend on the nitrogen content [13,18,19]. These experimental facts and other studies [20–22] lead to the conclusion that the incorporation of small amounts of nitrogen affect mainly the electronic structure of the conduction band without any significant effect on the valence band.

So far, two independent but rather complementary approaches are used to explain the unusual behavior of dilute nitrides: one is based on detailed band structure calculations from first principles [23–27], while the other is a phenomenological approach based on the experimentally observed band anticrossing effect in the conduction band [1,5]. The second approach (i.e., BAC model) is also supported by theoretical studies based on the tight-binding method [21,22,28,29], and currently this model is widely used to calculate conduction band dispersions in the dilute nitrides.

The BAC model assumes that N atoms, substituted into the group V elements, are randomly distributed in the crystal lattice and weakly coupled to extended states of the host semiconductor matrix [1,5,30]. The original BAC model developed for GaN_xAs_{1-x} alloys considers two sets of states: localized states of substitutional nitrogen atoms and extended states of the GaAs matrix conduction band. Later, the model was modified to consider a larger set of bands with a standard ***kp*** approach [31,32]. In the case of $GaN_xP_yAs_{1-x-y}$ alloys, the locations of the conduction band minima in the GaP_yAs_{1-y} matrix depend on the alloy composition, and, in the current case of $GaN_xP_{0.4}As_{0.6-x}$, all the high-symmetry conduction band minima interact with the close-lying N level.

Interaction of N-related states with a conduction band minimum is modeled by the BAC Hamiltonian using the perturbation theory:

$$H_{\mathrm{BAC}} = \begin{pmatrix} E_M(k) & C_{\mathrm{N}M}\sqrt{x} \\ C_{\mathrm{N}M}\sqrt{x} & E_{\mathrm{N}} \end{pmatrix}, \tag{1}$$

where $C_{\mathrm{N}M}$ is a constant, which depends on the semiconductor matrix, and x is the mole fraction of substitutional N atoms. $E_M(k)$ is the energy dispersion of the lowest conduction band of the III–V host, and E_{N} is the energy of N-related states, all referenced to the top of the valence band of the III–V semiconductor host.

According to the BAC Hamiltonian, Eq. (1), the interaction of dispersionless N-related states with the conduction band states results in a characteristic level anticrossing that leads to a splitting of the conduction band into two highly nonparabolic subbands, $E_-(k)$ and $E_+(k)$, which are given by Eq. (2):

$$E_{\pm}(k) = \frac{1}{2}\left[E_{\mathrm{N}} + E_M(k) \pm \sqrt{[E_{\mathrm{N}} - E_M(k)]^2 + 4C_{\mathrm{N}M}^2 x}\right]. \tag{2}$$

It has been shown previously that a similar approach can be applied to describe the BAC interaction with minima at the X and L points of the Brillouin zone. The only difference is that the coupling constant $C_{\mathrm{N}M}$ has to be modified, since the conduction band states lose the s-like character with the A_1 symmetry. It is observed that the interaction between N-related states and conduction band states at the boundary of Brillouin zone still exists for dilute nitrides [33,34]. Some experimental evidence of this interaction is provided by Seong, Mascarenhas, and Geisz using Raman scattering [33] and Perkins *et al.* using the electroreflectance technique [34]. Thus, a nonzero $C_{\mathrm{N}M}$ element is expected for electron states at the boundary of the Brillouin zone. It is found [4] that the $C_{\mathrm{N}M}(k)$ element can be expressed as

$$C_{\mathrm{N}M}(k) = \frac{C_{\mathrm{N}\Gamma}}{[1 + (ak)^2]^2}, \tag{3}$$

where a is the parameter of the order of lattice constant describing the spatial extent of the N localization wave function and $C_{\mathrm{N}\Gamma}$ is the $C_{\mathrm{N}M}(k)$ for $k = 0$, which should be determined from measurements of the band anticrossing interaction in the conduction band at the Γ point. Experimentally, it is observed that $C_{\mathrm{N}M}(k)$ at the X point is 3–4 times smaller than $C_{\mathrm{N}\Gamma}$ [4].

In order to find the optimal composition of GaNPAs alloys for IB solar cells, the BAC model is used to calculate energies of E_- and E_+ in GaNPAs alloys of various compositions. Results of these calculations are presented in Fig. 1. Material parameters used for these calculations are taken from Ref. [35], and BAC parameters (E_{N} and $C_{\mathrm{N}M}$) for $GaN_xP_yAs_{1-x-y}$ are calculated as a linear interpolation of the BAC parameters for GaNAs ($E_{\mathrm{N}} = 1.65$ eV and $C_{\mathrm{N}M} = 2.8$ eV [5,36]) and GaNP

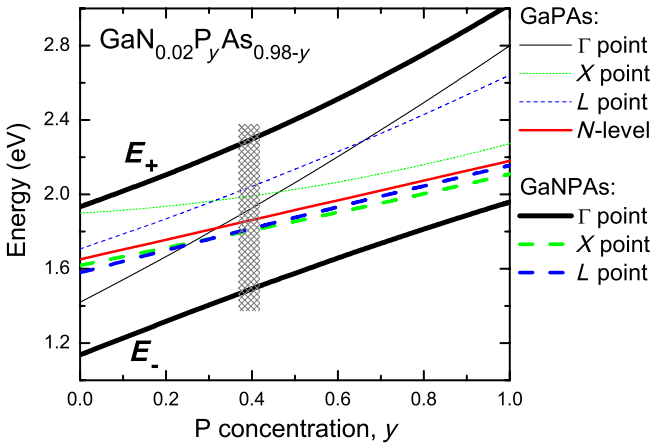

FIG. 1. Energy gap between the top of the valence band and the bottom of the conduction band at the Γ (solid black line), X (dashed green line), and L (dashed blue line) points for GaPAs (thin lines) and $GaN_{0.02}P_yAs_{0.98-y}$ (thick lines) alloys with various P concentrations. The solid red line shows the position of the nitrogen level in the GaPAs host.

($E_N = 2.18$ eV and $C_{NM} = 3.05$ eV [36]). Additionally, Fig. 1 also shows the composition dependence of the conduction band minima energies at different symmetry points in the GaPAs host. Indicated by the gray bar in Fig. 1, the nitrogen level falls below the conduction band minimum in GaP_yAs_{1-y} with y larger than ~0.4. The calculations presented in Fig. 1 show that the incorporation of 2% of nitrogen into such a host material leads to a splitting of the conduction band into E_+ and E_- subbands. The resulting band structure has three optical gaps with absorption edges suitable for an intermediate-band solar cell.

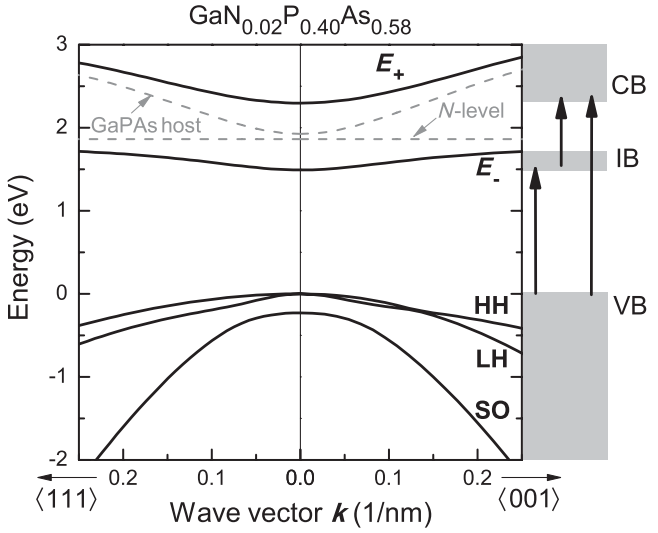

FIG. 2. Band structure of the $GaP_{0.4}As_{0.6}$ host (gray lines) obtained within the eight-band ***kp*** model and $GaN_{0.02}P_{0.40}As_{0.58}$ (black lines) calculated within the BAC model with the following parameters: $E_N = 1.86$ eV, $C_{N\Gamma} = 2.84$ eV, and $C_{NX} = C_{NL} = C_{N\Gamma}/4$.

Figure 2 shows the calculated dispersion relations for the conduction and the valence bands close to the Γ point of the Brillouin zone. The band structure of the $GaP_{0.4}As_{0.6}$ host (gray lines) is obtained within the eight-band ***kp*** Hamiltonian. The dispersion relations of $GaN_{0.02}P_{0.40}As_{0.58}$ (black lines) are calculated by using the BAC model. Figure 2 shows that the BAC-induced splitting of the conduction band results in the formation of a narrow IB that is well separated from the upper CB. Figure 3 shows the calculated density of states (DOS) of (a) GaN_xAs_{1-x} and (b) $GaN_xP_{0.4}As_{0.6-x}$ for different N content x. The dashed vertical lines indicate the position of the N level in the matrix materials. This is a band structure configuration envisioned for the intermediate-band solar cell concept that utilizes low-energy photons in a two-step absorption process via the intermediate band. The three absorption edges resulting from the optical transitions from VB to CB (~2.4 eV), from VB to IB (~1.5 eV), and IB to CB (~0.9 eV) are close to the band gap distribution for efficient solar power conversion under idealized conditions [7,8]. We also calculate the BAC interaction between N states and the extended states of the close-lying X and L minima. As is seen in Fig. 1, because of the much smaller coupling parameter C_{NM}, the splittings of these minima are

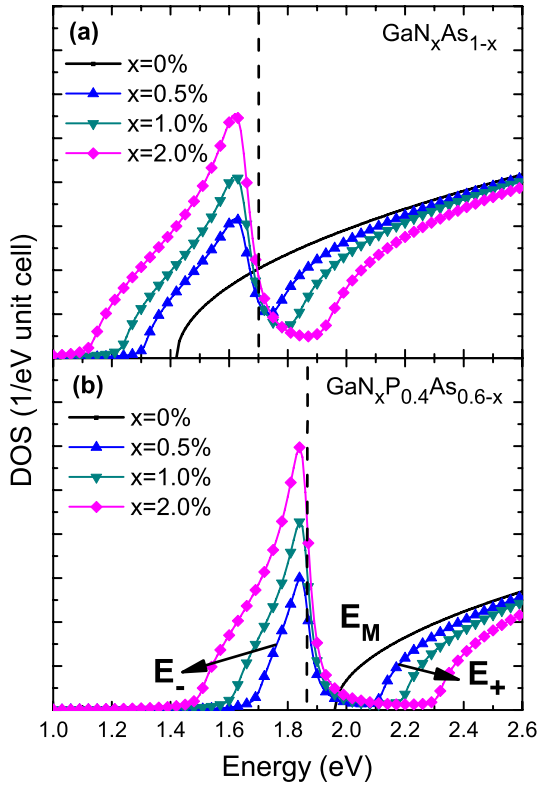

FIG. 3. Calculated DOS of (a) GaN_xAs_{1-x} and (b) $GaN_xP_{0.4}As_{0.6-x}$ for different N content x. The dashed vertical lines indicate the position of the N level in the matrix materials.

at least one order of magnitude smaller than the splitting at the Γ minimum and therefore can be safely ignored.

III. EXPERIMENTAL RESULTS AND DISCUSSION

In order to verify the above predictions and identify experimentally features related to IB formation in GaNPAs alloys, PR and absorption techniques are applied to study GaNPAs samples with variable N (0.56%–1.5%) and P (38%–45%) concentrations.

The samples are grown in a Varian Gen-II molecular beam epitaxy system modified to handle gas sources. Thermally cracked PH_3 and AsH_3 at 1000 °C and rf N plasma excited at 13.56 MHz are used for P, As, and N sources, respectively. Solid elemental Ga is used to generate a Ga atomic beam through an effusion cell. After a 0.3-μm-thick GaP buffer layer is grown at 580 °C, a 1.5-μm-thick linearly graded GaP_yAs_{1-y} (from $y = 1$ to ~0.4) and a 0.5-μm-thick GaPAs with uniform As content are grown at 520 °C. Then the top 0.5-μm-thick $GaN_xP_yAs_{1-x-y}$ layer is grown at 520 °C. In order to improve optical properties of GaNPAs layers, the samples are annealed at 900 °C for 60 s in 95% N_2 and 5% H_2 forming gas ambient.

The composition of the GaNPAs layers is measured by channeling Rutherford backscattering spectroscopy (c-RBS), together with nuclear reaction analysis (NRA). The fraction of substitutional nitrogen atoms in the films is obtained by comparing yields of the RBS and the NRA measurements in the random and channeling orientations. The channeling c-RBS shows that samples grown in such a structure are of good crystalline quality with a minimum channeling yield of approximately 5%. Channeling RBS and NRA reveals that the substitutional N fraction is $\geq 80\%$ for all samples. Relevant details on sample growth and their structural characterization can be found in Refs. [37,38].

For PR measurements, samples are excited by the 442-nm line from a HeCd laser, and the signal is detected by a Si detector using the lock-in technique. Absorption coefficients of the films are obtained by transmission and refection measurements using a Perkin Elmer Lambda 950 photospectrometer.

Figure 4 shows PR and absorption spectra measured at room temperature for GaPAs (reference sample) and GaNPAs samples (as-grown and annealed). PR resonances related to the energy gap (E_0) and the spin-orbit split ($E_0 + \Delta_{SO}$) transitions are observed for the reference sample. For GaNPAs samples, the E_- and E_+ transitions are visible instead of the E_0 transition. Additionally, the $E_- + \Delta_{SO}$ and $E_+ + \Delta_{SO}$ transitions are also visible in these samples. The spin-orbit splitting in N-free and N-containing alloys is the same within the experimental error and equals 283, 282, and 270 meV for GaPAs, as-grown GaNPAs, and annealed GaNPAs samples, respectively. This observation confirms that the incorporation of nitrogen into GaPAs host changes the CB without any significant effect on the VB. Very similar PR spectra are observed for other GaNPAs samples. However, as is shown in Fig. 5, in some of the samples a strong PR signal from GaPAs template interferes with optical transitions from the GaNPAs layer. The E_0 transition in the GaPAs template is easy to recognize, as it coincides with the absorption edge marked by the dashed vertical line in Figs. 4 and 5.

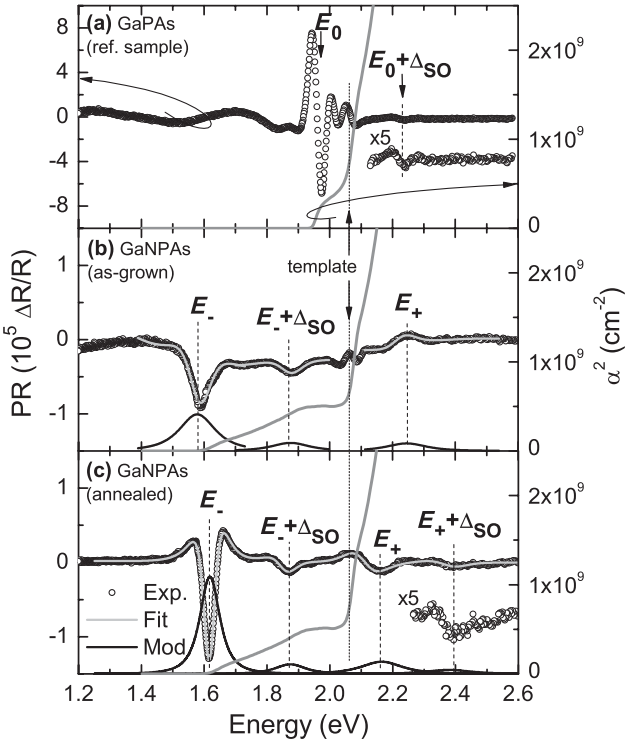

FIG. 4. Room temperature photoreflectance and absorption spectra for $GaP_{0.46}As_{0.54}$ (a), as-grown $GaN_{0.015}P_{0.445}As_{0.54}$ (b), and annealed $GaN_{0.015}P_{0.445}As_{0.54}$ (c) samples.

In order to extract energies of optical transitions in GaNPAs layers from PR spectra, these transitions are fitted by the Aspnes formula [39]

$$\frac{\Delta R}{R}(E) = \mathrm{Re}[Ce^{i\vartheta}(E - E_j + i\Gamma)^{-m}], \tag{4}$$

where $\frac{\Delta R}{R}(E)$ is the energy-dependent PR signal, C and ϑ are the amplitude and phase, respectively, of the resonance, E_j and Γ are the energy and the broadening parameter of the optical transition, respectively, and m depends on the type of optical transition and is assumed to be $m = 2.5$ in this case. The fitted curves are shown as thick gray lines in Figs. 4 and 5 together with the moduli of PR resonances, which are shown as solid black lines. The modulus of PR resonance (ρ) is obtained according to Eq. (5) with parameters taken from the fit:

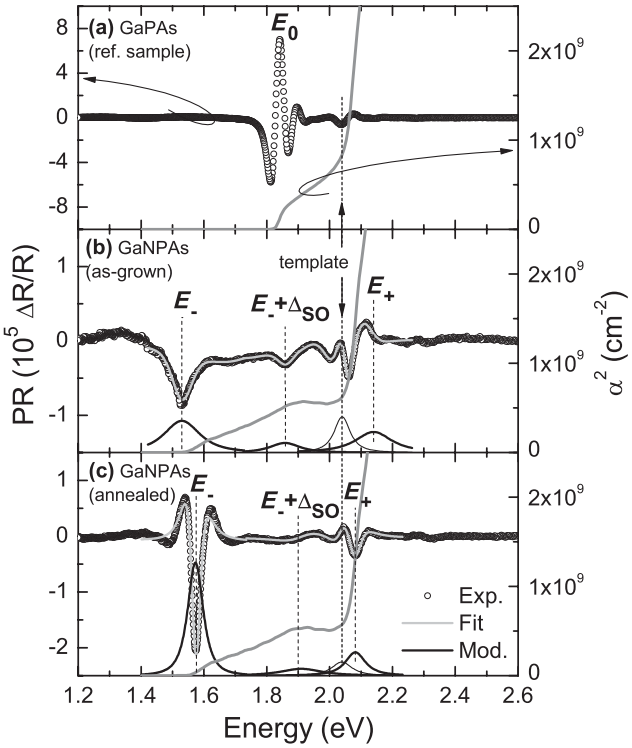

FIG. 5. Room temperature photoreflectance and absorption spectra for $GaP_{0.38}As_{0.62}$ (a), as-grown $GaN_{0.012}P_{0.38}As_{0.608}$ (b), and annealed $GaN_{0.012}P_{0.38}As_{0.608}$ (c) samples.

$$\Delta\rho(E) = \frac{|C|}{[(E-E_j)^2+\Gamma^2]^{m/2}}. \tag{5}$$

It is worth noting that postgrowth annealing influences the spectral position and strength of optical transitions in GaNPAs samples. By analyzing the moduli of PR transitions for as-grown and annealed samples, it is clearly visible that the E_- transition is slightly blueshifted while the E_+ transition is redshifted after annealing. Such a behavior of E_- and E_+ transitions is consistent with the reduction and/or passivation of substitutional N in GaNPAs during annealing. A blueshift of the E_- transition was also observed for GaInNAs layers, but in this material the blueshift phenomenon is mostly attributed to the change in the nitrogen nearest-neighbor environment from Ga rich to In rich [40–42]. For GaInNAs it has been reported that substitutional nitrogen atoms with different nearest-neighbor environments influence the coupling element C_{NM} in the BAC model and thus affect the energy gap [43]. It is also possible that energies of E_- and E_+ transitions can vary with the same nitrogen concentration due to a different nitrogen nearest-neighbor environment which influences the coupling element in GaNPAs alloys.

Thermal annealing is an often-used technique to improve the optical quality of dilute nitrides. As is shown in Figs. 4 and 5, a significant reduction of the linewidth is observed in the PR spectra of annealed GaNPAs layers. Narrowing of optical transitions in modulated reflectance spectra is also observed for other dilute nitrides [44] and is attributed to an improvement of the alloy homogeneity and/or reduction of point defects in these layers.

Figure 6 shows theoretical predictions of the transition energies from the valence band to E_- and E_+ subbands in $GaN_xP_yAs_{1-x-y}$ alloys with various nitrogen concentrations. The calculations are compared with experimental data for as-grown (solid points) and annealed (open points) GaNPAs samples. The predictions are compared to samples with three different P concentrations ($y = 0.38$, 0.40, and 0.44) as determined by RBS. Although there is an overall good agreement between the BAC calculations and the experiment, it is clearly visible that the agreement is better for the E_- rather than for the E_+ transition. This agreement is not surprising, as the E_+ transitions in some of the samples interfere with the optical transitions from the template and are more difficult to measure accurately. We also note that the accuracy of substitutional N fraction measured by c-RBS and c-NRA is approximately 15%, which is within the changes observed between as-grown and annealed samples.

The results in Fig. 6 confirm experimentally that $GaN_xP_{0.4}As_{0.6-x}$ alloys with approximately 1%–2% of N have a band structure suitable for IB solar cells. However, an important requirement for an efficient IBSC is a strong enough absorption for the optical transitions from the VB to IB and from the IB to CB. In the case of GaNPAs with the nitrogen level located below the GaPAs conduction band, the character of the IB is mostly determined by the highly localized N states, and the question arises as to whether there is strong enough optical coupling between the extended band states and the IB. The absorption spectra measured on different samples are shown in Fig. 7. As expected, changing P concentration from 38% to

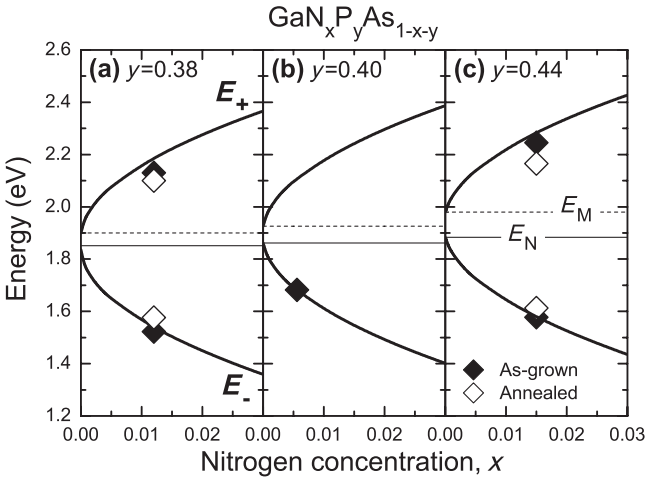

FIG. 6. Energies of the E_- and E_+ transitions for as-grown (solid points) and annealed (open points) GaNPAs layers, along with theoretical predictions obtained within the BAC model.

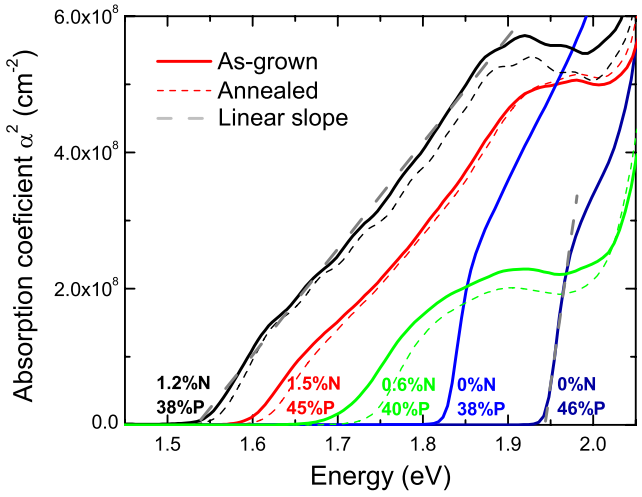

FIG. 7. Room temperature absorption spectra of Ga(N)PAs samples of various contents.

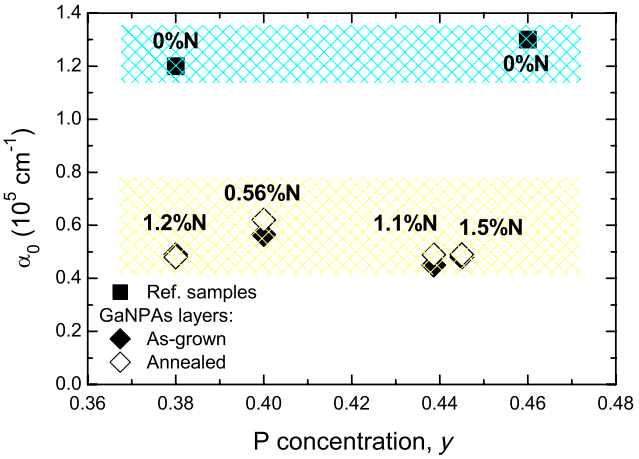

FIG. 8. Absorption coefficient α_0 determined for Ga(N)PAs alloys of various contents.

46% in N-free alloys changes the absorption edge E_0 to higher energy without affecting the shape of the edge. In the case of GaNPAs films, we observe a large downward shift of the absorption edge, indicating an onset of the transitions from the VB to IB (E_-). The low-energy optical absorption has a tendency to saturate at higher energies of about 1.8–2 eV with the saturation level dependent on the N content. This behavior reflects the fact that the nature of the IB states and thus also that of the dipole matrix element for the transitions from the VB to IB depends on the k vector. At small k's, the IB states have a large admixture of the s-like CB states that strongly couple to the p-like VB states. As shown in Fig. 2, at large k values the IB states approach E_N and become more localized with weaker optical coupling to the extended VB states. This effect results in the saturation of the optical absorption for the VB to IB transitions. In order to evaluate the absorption edge energy and the relative strength of the optical absorption from the spectra in Fig. 7, we use a simple formula for the photon energy E, dependent absorption coefficient

$$\alpha(E) = \alpha_0 \sqrt{\frac{E - E_g}{E_g}}, \tag{6}$$

where E_g is the energy gap and α_0 is a constant that is a measure of the strength of the optical absorption. The thick dashed lines in Fig. 7 represent the fits and are used to determine E_g and α_0. The values of α_0 for different samples are plotted in Fig. 8. It is clearly evident that the incorporation of nitrogen into the GaPAs host leads to the formation of an IB with an absorption coefficient of about 0.5×10^5 cm^{-1} for the VB $\rightarrow$ IB transition, which is only about 50%–60% smaller than the absorption coefficient for the VB $\rightarrow$ CB transition in the GaPAs host. This result indicates that the GaNPAs thin films have an optical absorption for VB to IB transitions strong enough to be used in thin-film IB solar cells. For example, >90% of incident light with photon energy larger than E_- can be absorbed by only a 0.5 μm thickness of GaNPAs.

IV. SUMMARY

We study the optical properties of $GaN_xP_yAs_{1-x-y}$ alloys in the whole P composition range. Calculations of the electronic band structure based on the BAC model indicate that dilute nitride GaNPAs with approximately 40% P has a band structure and optical properties suitable for application in intermediate-band solar cells. The predictions are experimentally tested on GaNPAs alloys with P content ranging from 38% to 45%. The energies of the optical transitions are in good agreement with the BAC calculations. Measurements of the optical absorption show a strong optical coupling between the valence and the intermediate band, which is a key requirement for the application of GaNPAs alloys in thin-film intermediate-band solar cells. The improvement of efficiency in such devices is associated with preserving the output voltage high enough and increasing the current of the solar cell by utilizing low-energy photons in a two-step absorption process via the intermediate band. Additional studies of intentionally doped alloys will be required to evaluate both the strength of the complementary IB to CB transitions and the charge transport in the conduction band to further evaluate the suitability of GaNPAs alloys for application in solar energy conversion devices.

ACKNOWLEDGMENTS

Sample growth by GSMBE at UCSD was supported by National Science Foundation Grants No. DMR-0907652 and No. DMR-1106369. RBS, NRA, absorption, and PR characterization performed at LBNL was supported by the Director, Office of Science, Office of Basic Energy

Sciences, Materials Sciences and Engineering Division, of the U.S. Department of Energy under Contract No. DE-AC02-05CH11231. In addition, R. K. acknowledges the support within the grant "Mobilnosc Plus" from the MNiSzW. A. V. L. acknowledges support from an NSF Graduate Research Fellowship.

[1] W. Shan, W. Walukiewicz, J. W. Ager III, E. E. Haller, J. F. Geisz, D. J. Friedman, J. M. Olson, and S. R. Kurtz, Band anticrossing in GaInNAs alloys, Phys. Rev. Lett. **82**, 1221 (1999).

[2] K. M. Yu, W. Walukiewicz, J. W. Ager III, D. Bour, R. Farshchi, O. D. Dubon, S. X. Li, I. D. Sharp, and E. E. Haller, Multiband GaNAsP quaternary alloys, Appl. Phys. Lett. **88**, 092110 (2006).

[3] W. Walukiewicz, W. Shan, K. M. Yu, J. W. Ager III, E. E. Haller, I. Miotkowski, M. J. Seong, H. Alawadhi, and A. K. Ramdas, Interaction of localized electronic states with the conduction band: Band anticrossing in II-VI semiconductor ternaries, Phys. Rev. Lett. **85**, 1552 (2000).

[4] J. Wu, W. Walukiewicz, K. M. Yu, J. W. Ager III, E. E. Haller, Y. G. Hong, H. P. Xin, and C. W. Tu, Band anticrossing in $GaP_{1-x}N_x$ alloys, Phys. Rev. B **65**, 241303(R) (2002).

[5] J. Wu, W. Shan, and W. Walukiewicz, Band anticrossing in highly mismatched III–V semiconductor alloys, Semicond. Sci. Technol. **17**, 860 (2002).

[6] K. Alberi, O. D. Dubon, W. Walukiewicz, K. M. Yu, K. Bertulis, and A. Krotkus, Valence band anticrossing in $GaBi_xAs_{1-x}$, Appl. Phys. Lett. **91**, 051909 (2007).

[7] A. Luque and A. Marti, Increasing the efficiency of ideal solar cells by photon induced transitions at intermediate levels, Phys. Rev. Lett. **78**, 5014 (1997).

[8] A. Luque and A. Marti, The intermediate band solar cell: Progress toward the realization of an attractive concept, Adv. Mater. **22**, 160 (2010).

[9] K. M. Yu, W. Walukiewicz, J. Wu, W. Shan, J. W. Beeman, M. A. Scarpulla, O. D. Dubon, and P. Becla, Diluted II-VI oxide semiconductors with multiple band gaps, Phys. Rev. Lett. **91**, 246403 (2003).

[10] N. Lopez, L. A. Reichertz, K. M. Yu, K. Campman, and W. Walukiewicz, Engineering the electronic band structure for multiband solar cells, Phys. Rev. Lett. **106**, 028701 (2011).

[11] N. Ahsan, N. Miyashita, M. M. Islam, K. M. Yu, W. Walukiewicz, and Y. Okada, Effect of Sb on GaNAs intermediate band solar cells, IEEE J. Photovoltaics, **3**, 730 (2013); Two-photon excitation in an intermediate band solar cell structure, Appl. Phys. Lett. **100**, 172111 (2012).

[12] T. Tanaka, M. Miyabara, Y. Nagao, K. Saito, Q. Guo, M. Nishio, K. M. Yu, and W. Walukiewicz, Photocurrent induced by two-photon excitation in ZnTeO intermediate band solar cells, Appl. Phys. Lett. **102**, 052111 (2013).

[13] J. D. Perkins, A. Mascarenhas, Y. Zhang, J. F. Geisz, D. J. Friedman, J. M. Olson, and S. R. Kurtz, Nitrogen-activated transitions, level repulsion, and band gap reduction in $GaAs_{1-x}N_x$ with $x < 0.03$, Phys. Rev. Lett. **82**, 3312 (1999).

[14] K. M. Yu, W. Walukiewicz, J. W. Beeman, M. A. Scarpulla, O. Dubon, M. R. Pillai, and M. Aziz, Enhanced nitrogen incorporation by pulsed laser annealing of GaN_xAs_{1-x} formed by N implantation, Appl. Phys. Lett. **80**, 3958 (2002).

[15] A. Grau, T. Passow, and M. Hetterich, Temperature dependence of the GaAsN conduction band structure, Appl. Phys. Lett. **89**, 202105 (2006).

[16] S. Procz, M. Fiederle, M. Kunzer, K. Köhler, and J. Wagner, Band anticrossing in diluted $Al_xGa_{1-x}As_{1-y}Ny$ $(x \leqslant 0.37, y \leqslant 0.04)$, J. Appl. Phys. **103**, 073103 (2008).

[17] K. I. Lin, T. S. Wang, J. T. Tsai, and J. S. Hwang, Temperature-dependent parameters of band anticrossing in InGaPN alloys, J. Appl. Phys. **104**, 016109 (2008).

[18] R. Kudrawiec, J. Misiewicz, Q. Zhuang, A. M. R. Godenir, and A. Krier, Photoreflectance study of the energy gap and spin-orbit splitting in InNAs alloys, Appl. Phys. Lett. **94**, 151902 (2009).

[19] R. Kudrawiec, M. Latkowska, J. Misiewicz, Q. Zhuang, A. M. R. Godenir, and A. Krier, Photoreflectance study of N-and Sb-related modifications of the energy gap and spin-orbit splitting in InNAsSb alloys, Appl. Phys. Lett. **99**, 011904 (2011).

[20] C. Skierbiszewski, P. Perlin, P. Wisniewski, W. Knap, T. Suski, W. Walukiewicz, W. Shan, K. M. Yu, J. W. Ager, E. E. Haller, J. F. Gaisz, and J. M. Olson, Large, nitrogen-induced increase of the electron effective mass in $In_yGa_{1-y}N_xAs_{1-x}$, Appl. Phys. Lett. **76**, 2409 (2000).

[21] E. P. O'Reilly, A. Lindsay, S. Tomic, and M. Kamal-Saadi, Tight-binding and ***kp*** models for the electronic structure of Ga(In)NAs and related alloys, Semicond. Sci. Technol. **17**, 870 (2002).

[22] A. Lindsay and E. P. O'Reilly, Unification of the band anticrossing and cluster-state models of dilute nitride semiconductor alloys, Phys. Rev. Lett. **93**, 196402 (2004).

[23] T. Mattila, S. H. Wei, and A. Zunger, Localization and anticrossing of electron levels in $GaAs_{1-x}N_x$ alloys, Phys. Rev. B **60**, R11245 (1999).

[24] E. D. Jones, N. A. Modine, A. A. Allerman, S. R. Kurtz, A. F. Wright, S. T. Tozer, and X. Wei, Band structure of $In_xGa_{1-x}As_{1-y}N_y$ alloys and effects of pressure, Phys. Rev. B **60**, 4430 (1999).

[25] P. R. C. Kent and A. Zunger, Theory of electronic structure evolution in GaAsN and GaPN alloys, Phys. Rev. B **64**, 115208 (2001).

[26] P. R. C. Kent, L. Bellaiche, and A. Zunger, Pseudopotential theory of dilute III–V nitrides, Semicond. Sci. Technol. **17**, 851 (2002).

[27] N. G. Szwacki and P. Boguslawski, GaAs:N vs GaAs:B alloys: Symmetry-induced effects, Phys. Rev. B **64**, 161201 (2001).

[28] A. Lindsay and E. P. O'Reilly, Theory of enhanced bandgap non-parabolicity in GaN_xAs_{1-x} and related alloys, Solid State Commun. **112**, 443 (1999).

[29] A. Lindsay and E. P. O'Reilly, Influence of nitrogen resonant states on the electronic structure of GaN_xAs_{1-x}, Solid State Commun. **118**, 313 (2001).

[30] W. Shan, W. Walukiewicz, K. M. Yu, J. W. Ager III, E. E. Haller, J. F. Geisz, D. J. Friedman, J. M. Olson, S. R. Kurtz,

H. P. Xin, and C. W. Tu, Band anticrossing in III–N–V alloys, Phys. Status Solidi (b) **223**, 75 (2001).

[31] S. Tomic, E. P. O'Reilly, R. Fehse, S. J. Sweeney, A. R. Adams, A. D. Andreev, S. A. Choulis, T. J. Hosea, and H. Riechert, Theoretical and experimental analysis of 1.3-μm InGaAsN/GaAs lasers, IEEE J. Sel. Top. Quantum Electron. **9**, 1228 (2003).

[32] M. Gladysiewicz, R. Kudrawiec, J. M. Miloszewski, P. Weetman, J. Misiewicz, and M. Wartak, Band structure and the optical gain of GaInNAs/GaAs quantum wells modeled within 10-band and 8-band ***kp*** model, J. Appl. Phys. **113**, 063514 (2013).

[33] M. J. Seong, A. Mascarenhas, and J. F. Geisz, $\Gamma - L - X$ mixed symmetry of nitrogen-induced states in $GaAs_{1-x}N_x$ probed by resonant Raman scattering, Appl. Phys. Lett. **79**, 1297 (2001).

[34] J. D. Perkins, A. Mascarenhas, J. F. Geisz, and D. J. Friedman, Conduction-band-resonant nitrogen-induced levels in $GaAs_{1-x}N_x$ with $x < 0.03$, Phys. Rev. B **64**, 121301 (2001).

[35] I. Vurgaftman, J. R. Meyer, and L. R. Ram-Mohan, Band parameters for III–V compound semiconductors and their alloys, J. Appl. Phys. **89**, 5815 (2001).

[36] I. Vurgaftman, and J. R. Meyer, Band parameters for nitrogen-containing semiconductors, J. Appl. Phys. **94**, 3675 (2003).

[37] Y.-J. Kuang, S.-W. Chen, H. Li, S. K. Sinha, and C. W. Tu, Growth of $GaN_xAs_yP_{1-x-y}$ alloys on GaP(100) by gas-source molecular beam epitaxy, J. Vac. Sci. Technol. B **30**, 02B121 (2012).

[38] Y. J. Kuang, K. M. Yu, R. Kudrawiec, A. V. Luce, M. Ting, W. Walukiewicz, and C. W. Tu, GaNAsP: An intermediate band semiconductor grown by gas-source molecular beam epitaxy, Appl. Phys. Lett. **102**, 112105 (2013).

[39] D. E. Aspnes, Third-derivative modulation spectroscopy with low-field electroreflectance, Surf. Sci. **37**, 418 (1973).

[40] P. J. Klar, H. Grüning, J. Koch, S. Schäfer, K. Volz, W. Stolz, W. Heimbrodt, A. M. Kamal Saadi, A. Lindsay, and E. P. O'Reilly, (Ga, In)(N, As)-fine structure of the band gap due to nearest-neighbor configurations of the isovalent nitrogen, Phys. Rev. B **64**, 121203(R) (2001).

[41] R. Kudrawiec, G. Sek, J. Misiewicz, D. Gollub, and A. Forchel, Explanation of annealing-induced blueshift of the optical transitions in GaInAsN/GaAs quantum wells, Appl. Phys. Lett. **83**, 2772 (2003).

[42] R. Kudrawiec, E.-M. Pavelescu, J. Wagner, G. Sęk, J. Misiewicz, M. Dumitrescu, J. Konttinen, A. Gheorghiu, and M. Pessa, Photoreflectance evidence of multiple band gaps in dilute GaInNAs layers lattice-matched to GaAs, J. Appl. Phys. **96**, 2576 (2004).

[43] J. Y. Duboz, J. A. Gupta, Z. R. Wasilewski, J. Ramsey, R. L. Williams, G. C. Aers, B. J. Riel, and G. I. Sproule, Band-gap energy of $In_xGa_{1-x}N_yAs_{1-y}$ as a function of N content, Phys. Rev. B **66**, 085313 (2002).

[44] R. Kudrawiec, P. Poloczek, J. Misiewicz, H. P. Bae, T. Sarmiento, S. R. Bank, H. B. Yuen, M. A. Wistey, and J. S. Harris, Contactless electroreflectance of GaInNAsSb/GaNAs/GaAs quantum wells emitting at 1.5–1.65 μm: Broadening of the fundamental transition, Appl. Phys. Lett. **94**, 031903 (2009).